# Supporting Information

## Kirby et al. 10.1073/pnas.1422448112

### SI Methods

**NSPC Isolation.** NSPCs were isolated from adult (6–7 wk old) hippocampus and maintained on plates coated with poly-D-lysine (Sigma) and laminin (Invitrogen) as described by Babu et al. (1). For WT NSPC isolations, two separate lines were used throughout the study: one from five pooled C57/Bl6 male mice and one from five pooled C57/Bl6 female mice. No differences between NSPCs isolated from males and females were found. All other NSPC lines were isolated from mixed-sex pools of five to six mice.

For the bulk sphere assay, after 4 d of treatment in an adherent monolayer, NSPCs were passaged and replated in uncoated plates at 3,000 cells per well for sphere growth. Spheres were fed after 2 d with a full dose of EGF/FGF2, passaged after 4 d using Cell Dissociation Buffer (Gibco), and then replated at 3,000 cells per well. Sphere number and size were quantified using a CellAvista automated microscope system (Roche).

For the neural colony-forming cell (NCFC) assay (Stem Cells, Inc.), after 4 d of treatment in an adherent monolayer, NSPCs were passaged and plated in the NCFC assay at 30,000 cells per well. Colonies were quantified by a blinded observer as per the manufacturer's instructions.

**Mice.** All mice were housed on a 12-h light/dark cycle with lights on at 0630 hours in the Veterans Administration Palo Alto Animal Facility. Food and water were available ad libitum. $VEGF^{fl}$ mice were provided by Genentech, Inc (2). $NestinCreER^{T2}$ mice were obtained from the The Jackson Laboratory (strain 01621) (3), as were R26-enhanced YFP reporter mice (strain 006148). VEGF-GFP mice were a gift from Brian Seed, Harvard University, Cambridge, MA (4). BrdU (Sigma) and EdU (Invitrogen) were injected i.p. at 150 mg/kg (5). TAM (Sigma) in sunflower oil was injected i.p. at 180 $mg{\cdot}kg{\cdot}d^{-1}$ for 3 or 5 d. One control mouse and one knockdown mouse were eliminated from cohort 2 due to abnormal body weight change after TAM treatment. For longer treatment, TAM was administered via diet (Harlan) as described by Welle et al. (6) and Kiermayer et al. (7) to reduce mortality (8).

**Qualitative and Quantitative Assessment of RNA.** The DG and SVZ were dissected from PBS-perfused mice, flash-frozen on dry ice, and stored at −80 °C. Adherent NSPCs were harvested using Accutase (Stem Cells, Inc.), and cell pellets were stored at −80 °C. RNA was extracted using an RNeasy Mini Kit (Qiagen) according to the manufacturer's instructions. A total of 250–500 ng of RNA was treated with DNase I (Invitrogen) and then converted to cDNA using the SuperScript III First Strand Synthesis System (Invitrogen). cDNA was diluted 1:5 in water. For qualitative PCR, 10 μL of cDNA was amplified using AmpliTaq Gold DNA Polymerase (Applied BioSystems) and primers for specific transcripts (Table S1). Amplified products were visualized on a 2% (wt/vol) agarose gel with ethidium bromide under UV illumination. Real-time quantitative PCR was performed using SYBR Green I Master mix (Roche) on a LightCycler 480 (Roche). Primers were designed to span exons (Table S1), and melting curves were used to confirm the purity of the amplified product. Cycle threshold (Ct) values in NSPCs were normalized to the HSP60 housekeeping gene except in differentiation experiments, where MAPK3 was used. Ct values for tissue were normalized to actin. δδCT values were used to yield fold change in mRNA over control in each experiment.

**Lentivirus Cloning.** pLM-CMV-R-Cre from Addgene (no. 27546, mCherry-Cre) was digested with RSRII and Sal1HF (New England Biosciences) and then blunt-end–ligated using T4 DNA polymerase followed by T4 DNA ligase (New England Biosciences) to create the mCherry lentiviral vector. Viral plasmids were packaged in vesicular stomatitis virus-glycoprotein G (VSV-G) lentivirus by the Stanford Gene Vector and Virus Core. Titer was determined in NSPCs as the minimal amount needed for ∼100% mCherry expression after 48 h.

**Immunostaining.** For immunocytochemistry, NSPCs on coated slides or wells were fixed with 4% (wt/vol) paraformaldehyde (PFA) for 10 min and then stained using standard procedures (9) (Table S2). For BrdU studies, NSPCs were given 20 μM BrdU 2 h before fixation. The number of $BrdU^+$ cells and the intensity of VEGFR2 staining were quantified by a CellAvista automated microscope.

All brains were harvested by perfusion with sterile PBS, followed by 24 h of postfixation in 4% PFA at +4 °C. Brains were equilibrated in 30% (wt/vol) sucrose in PBS, sliced in a 1:12 series of 40-μm coronal slices on a freezing microtome, and stored in cryoprotectant at −20 °C. Antibody staining was performed using standard procedures (9) (Table S2). All sections were mounted on Superfrost Plus microscope glass slides (Fisher Scientific) and protected with Prolong Gold antifading medium (Invitrogen).

**Western Blots.** For Western blots, NSPCs were plated in an adherent monolayer at a density appropriate for yielding 70–80% confluency at harvest. At harvest, cells were lysed with RIPA Lysis and Extraction buffer (Pierce) with Halt Protease and Phosphatase Inhibitor (Thermo Scientific) on ice, and total protein concentration was quantified using a bicinchoninic acid kit (Pierce). Lysates were run on 4–12% Bis-Tris gels in 1× NuPage MOPS SDS running buffer (Invitrogen) at 120 V for 2 h. Gels were transferred to nitrocellulose membrane overnight in 20% (vol/vol) methanol in NuPage Transfer Buffer (Invitrogen) at 4 °C. Membranes were blocked and then incubated in primary antibody overnight at 4 °C (Table S2). Proteins were visualized and quantified on a LI-COR Odyssey IR imaging system.


1. Babu H, et al. (2011) A protocol for isolation and enriched monolayer cultivation of neural precursor cells from mouse dentate gyrus. *Front Neurosci* 5:89.
2. Gerber HP, et al. (1999) VEGF is required for growth and survival in neonatal mice. *Development* 126(6):1149–1159.
3. Lagace DC, et al. (2007) Dynamic contribution of nestin-expressing stem cells to adult neurogenesis. *J Neurosci* 27(46):12623–12629.
4. Fukumura D, et al. (1998) Tumor induction of VEGF promoter activity in stromal cells. *Cell* 94(6):715–725.
5. Mandyam CD, Harburg GC, Eisch AJ (2007) Determination of key aspects of precursor cell proliferation, cell cycle length and kinetics in the adult mouse subgranular zone. *Neuroscience* 146(1):108–122.
6. Welle S, Burgess K, Thornton CA, Tawil R (2009) Relation between extent of myostatin depletion and muscle growth in mature mice. *Am J Physiol Endocrinol Metab* 297(4): E935–E940.
7. Kiermayer C, Conrad M, Schneider M, Schmidt J, Brielmeier M (2007) Optimization of spatiotemporal gene inactivation in mouse heart by oral application of tamoxifen citrate. *Genesis* 45(1):11–16.
8. Koitabashi N, et al. (2009) Avoidance of transient cardiomyopathy in cardiomyocyte-targeted tamoxifen-induced MerCreMer gene deletion models. *Circ Res* 105(1):12–15.
9. Kirby ED, et al. (2013) Acute stress enhances adult rat hippocampal neurogenesis and activation of newborn neurons via secreted astrocytic FGF2. *eLife* 2:e00362.

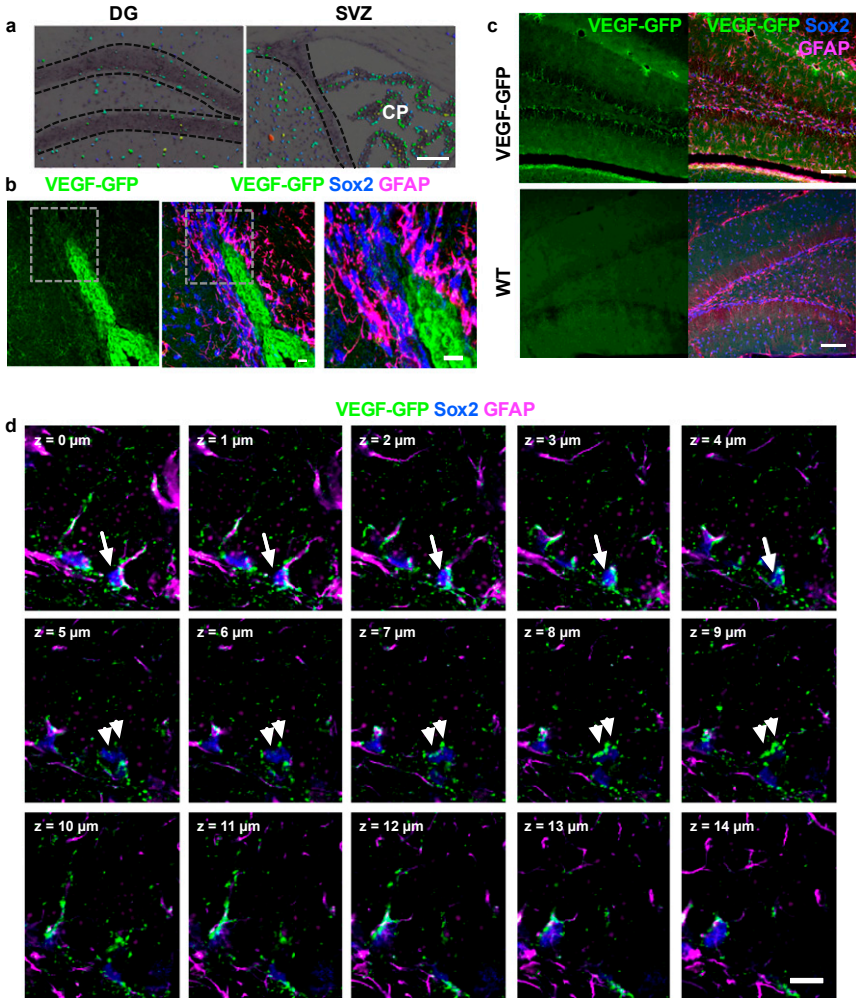


**Fig. S1.** VEGF in situ hybridization and VEGF-GFP images. (*A*) WT mouse DG (*Left*) and SVZ (*Right*) in situ hybridization for VEGF from the Allen Brain Atlas is shown in gray, with expression levels in the highlighted overlay. VEGF expression was found throughout the DG, including the neurogenic SGZ. The SVZ, in contrast, showed very few VEGF-expressing cells. The CP showed many VEGF-expressing cells. (Scale bar: 100 µm.) (*B*) VEGF-GFP expression in the SVZ. The boxes indicate areas shown to the right. (Scale bars: 10 µm.) (*C*) No GFP puncta were found in a WT mouse. (Scale bars: 100 µm.) (*D*) Series of 1-µm slices showing $GFP^+$ puncta colabeling with GFAP in an RGL (arrow) and $GFP^+$ puncta surrounding $Sox2^+$ TAPs (arrowheads). The z-level relative to first section is shown. (Scale bar: 10 µm.)

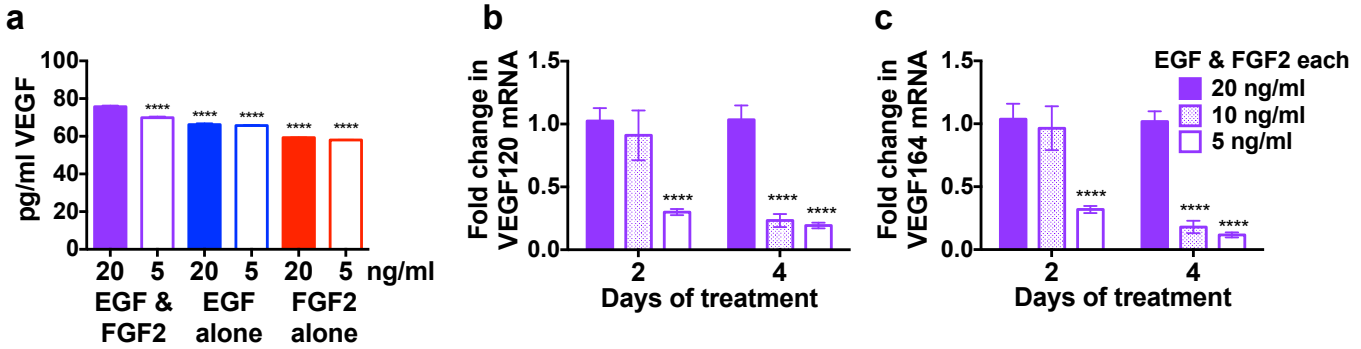


**Fig. S2.** NSPC-VEGF secretion depends on growth factor environment. (*A*) Adult NSPCs decreased VEGF secretion as measured by ELISA after 2 d in reduced EGF/FGF2 concentrations (ANOVA, $P < 0.0001$; $n$ = five wells per group per experiment; two experiments). (*B* and *C*) Reducing EGF and FGF2 levels decreased levels of VEGF120 and VEGF164 within 2 d. mRNA levels were normalized to the HSP60 housekeeping gene and expressed relative to 0 d of differentiation (VEGF120, two-way ANOVA: interaction, $P = 0.0059$; day, $P = 0.0054$; EGF/FGF2, $P < 0.0001$; VEGF164, two-way ANOVA: interaction, $P = 0.0011$; day, $P = 0.0002$; EGF/FGF2, $P < 0.0001$; $n = 3$ wells per group per experiment; two experiments). ****$P < 0.0001$, post hoc Dunnett's tests. Data represent mean ± SEM.

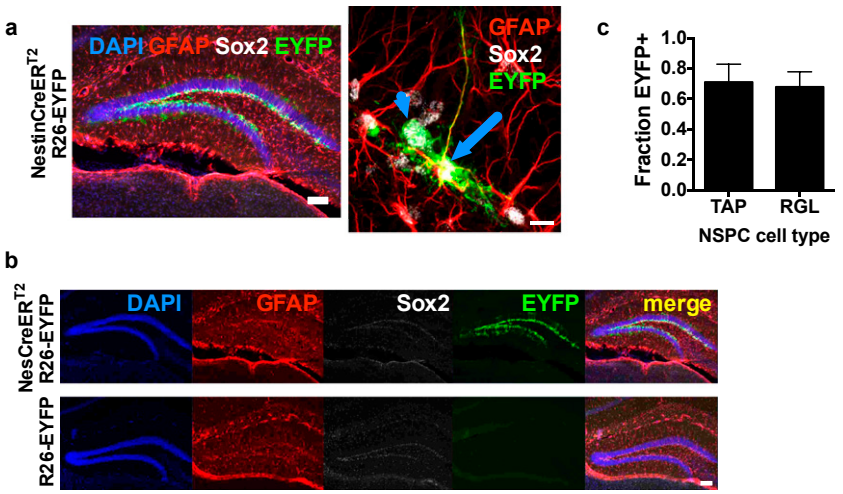


**Fig. S3.** TAM treatment in NestinCreER$^{T2}$ mice drives recombination in TAPs and RGL stem cells. (*A*) Adult NestinCreER$^{T2+}$;R26-enhanced YFP (EYFP) mice were treated with TAM for 5 d and then perfused 2 d after the last injection. An example image of EYFP$^{+}$ recombined NSPCs costained for Sox2, GFAP, and Hoechst (DAPI) is shown (*Left*), as well as an image with higher magnification (*Right*). Sox2$^{+}$ TAPs (blue arrowhead) and Sox2$^{+}$/GFAP$^{+}$ RGLs (blue arrow) both expressed EYFP. (Scale bars: *Left*, 100 μm; *Right*, 10 μm.) (*B*) Example images comparing EYFP labeling with Hoechst (DAPI), Sox2, and GFAP in a NestinCreER$^{T2}$;R26-EYFP mouse (*Top*) vs. an R26-EYFP mouse (*Bottom*). No EYFP fluorescence was observed in the R26-EYFP–only mouse. (Scale bar: 100 μm.) (*C*) Quantification of the proportion of TAPs and RGL stem cells expressing EYFP in NestinCreER$^{T2}$;R26-EYFP mice ($n = 3$).

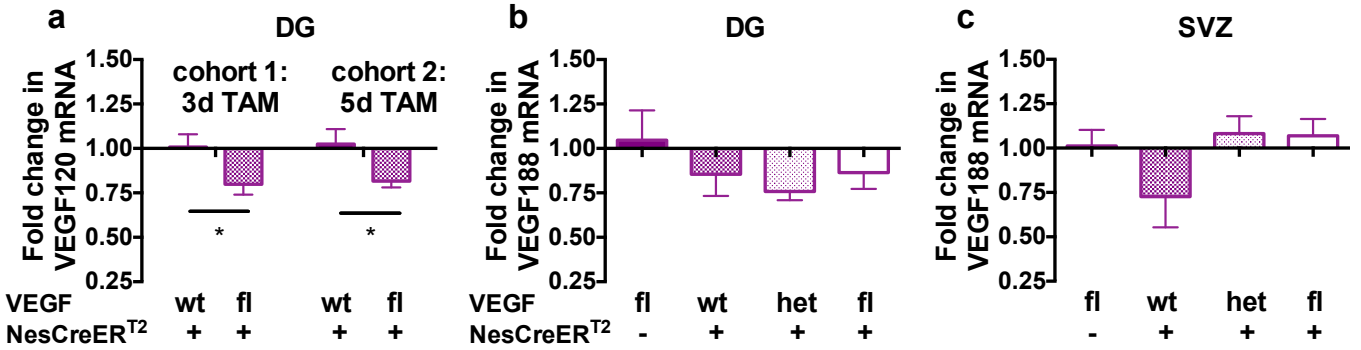


**Fig. S4.** NSPC-VEGF knockdown across cohorts and VEGF transcripts. (*A*) Two separate cohorts were treated with TAM for 3 d (cohort 1) or 5 d (cohort 2), and DG was dissected 1 wk after initiation of TAM treatment. VEGF-iKD (cohorts 1 and 2, $n = 4$) mice had significantly less VEGF120 mRNA than VEGF$^{wt/wt}$; NestinCreER$^{T2+}$ control mice (cohort 1, $n = 4$; cohort 2, $n = 3$) (two-way ANOVA: interaction, $P = 0.99$; cohort, $P = 0.79$; genotype, $P = 0.0073$). *$P < 0.05$, Fisher's least significant difference post hoc tests. Data represent mean ± SEM normalized to the actin housekeeping gene relative to control. (*B* and *C*) VEGF188 mRNA did not change with VEGF knockdown in NSPCs in the DG or SVZ, respectively. Data represent mean ± SEM normalized to the actin housekeeping gene, relative to Con (ANOVA, $P = 0.36$ in DG and $P = 0.23$ in SVZ). fl, homozygous floxed; het, heterozygous floxed.

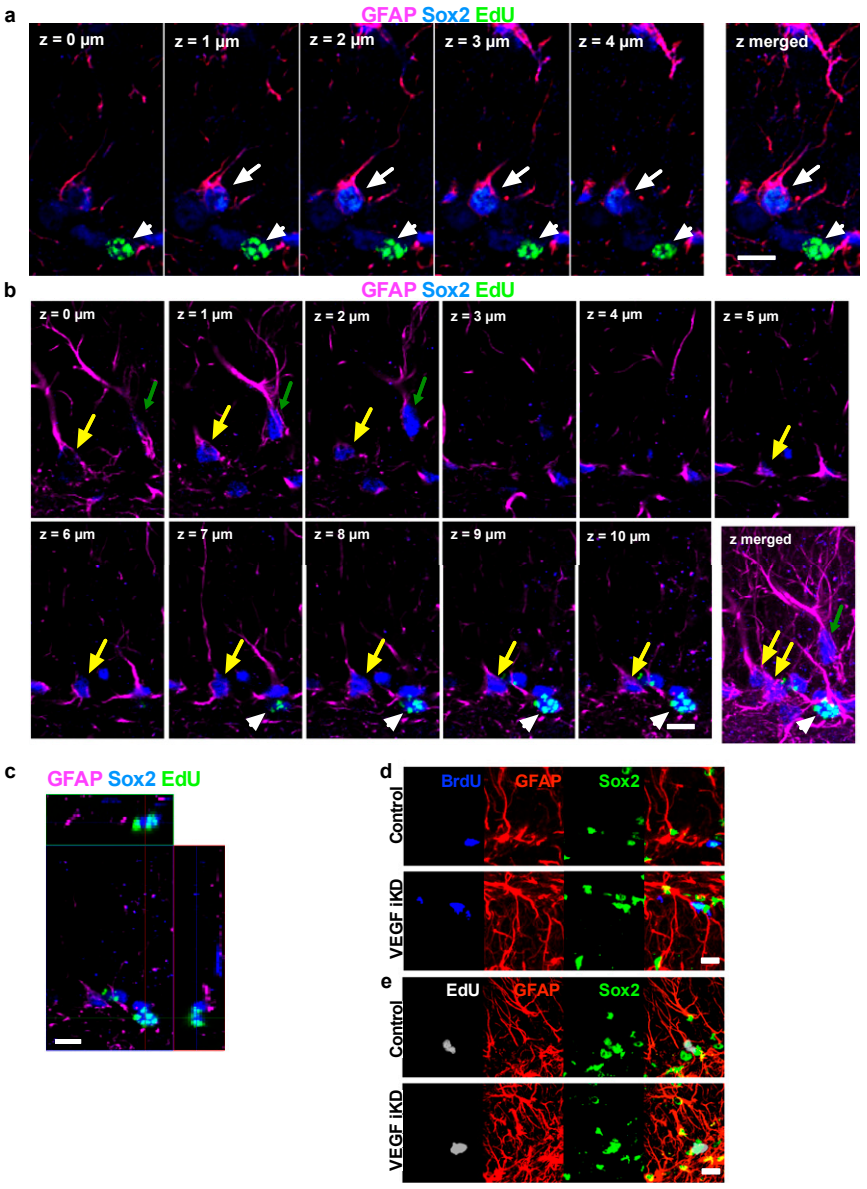


**Fig. S5.** (*A*) Series of 1-μm slices showing an example proliferating EdU$^+$/GFAP$^+$/Sox2$^+$ RGL (arrow) and an EdU$^+$/Sox2$^+$ proliferating TAP (arrowhead) from the 4-d time point (Fig. 4 *A* and *D*). (Scale bar: 10 μm.) (*Far Right*) Z-merged image is a maximum intensity merging of z-slices 0–4. The z-level relative to first section is shown. (*B*) Series of 1-μm slices showing example GFAP$^+$/Sox2$^+$ RGLs, GFAP$^+$/Sox2$^+$ astrocytes, and an EdU$^+$/Sox2$^+$ proliferating TAP. Large yellow arrows point to two different RGLs. The small green arrow points to a GFAP$^+$ astrocyte. The white arrowhead points to an EdU$^+$/Sox2$^+$ proliferating TAP. The z-merged image on the far right is a maximum intensity merging of z-slices 0–10. Z-level relative to first section. (Scale bar: 10 μm.) (*C*) Orthogonal image of a single 1-μm z-slice showing colocalization of Sox2 with EdU in a proliferating TAP from *A*. Images in *B* and *C* are from a control mouse treated with three rounds of TAM (also shown in Fig. S6). (Scale bar: 10 μm.) (*D*) Example image of Sox2, GFAP, and BrdU labeling in mice 21 d after TAM. (Scale bar: 10 μm.) (*E*) Example image of Sox2, GFAP, and EdU labeling in mice 60 d after TAM. (Scale bar: 10 μm.)

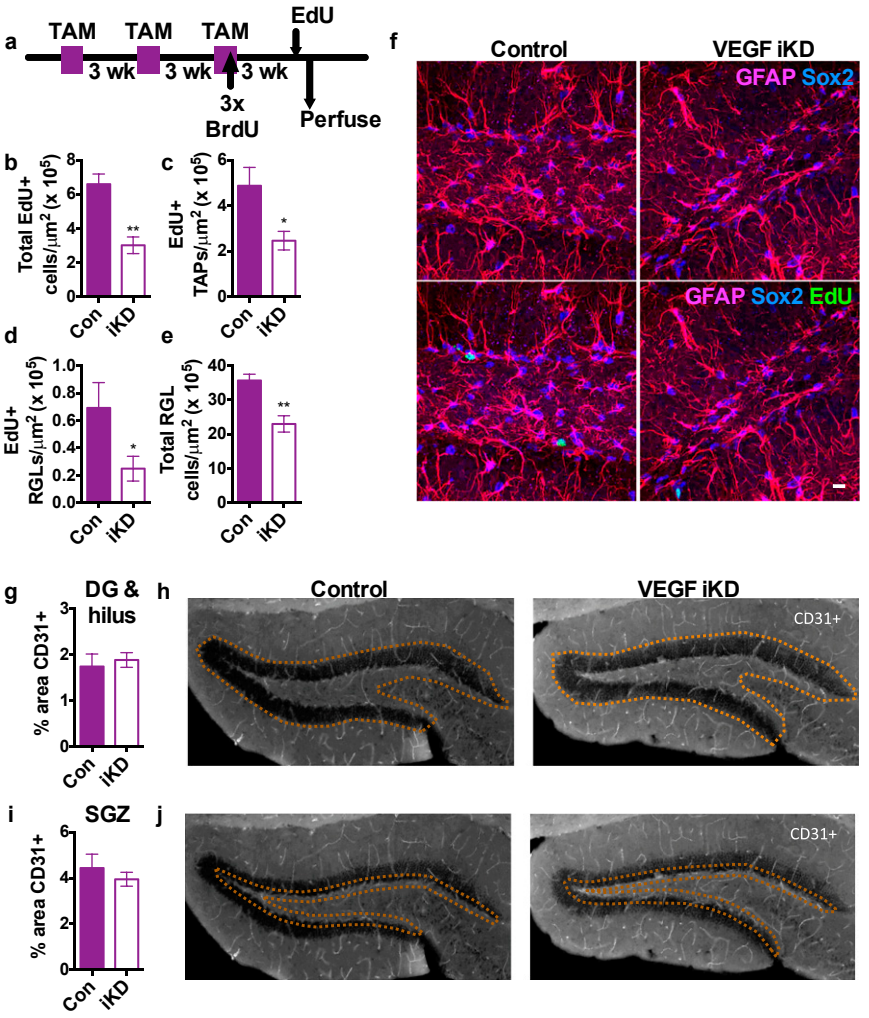


**Fig. S6.** Loss of NSPC-derived VEGF impairs NSPC maintenance in vivo. (*A*) Adult Con ($n = 4$) and VEGF-iKD ($n = 6$) mice were treated with TAM for 5 d, three times over 12 wk. BrdU was injected once per day for 3 d 3 wk before perfusion, whereas EdU was injected once 2 h before perfusion. (*B*) VEGF-iKD reduced the total number of proliferating EdU$^+$ cells in the SGZ. $^{**}P = 0.0016$, *t* test. This decrease in proliferation was found in the Sox2$^+$ TAPs (*C*; $^*P = 0.0185$, *t* test) and the Sox2$^+$/GFAP$^+$ RGL stem cells (*D*; $^*P = 0.0429$, *t* test). (*E*) Total number of RGL stem cells was also decreased by VEGF-iKD ($^{**}P = 0.0049$, *t* test). (*F*) Example images of EdU, Sox2, and GFAP in control and VEGF-iKD mice. (Scale bar: 10 μm.) (*G*) CD31$^+$ area in Con and iKD mice DG and hilus given three rounds of TAM over 12 wk was not different. (*H*) Example images of CD31$^+$ staining. The dashed area is the area quantified. (*I*) CD31$^+$ area in Con and iKD mice SGZ given three rounds of TAM over 12 wk was not different. (*J*) Example images of CD31$^+$ staining from *B*, but with the dashed area showing the SGZ area quantified.

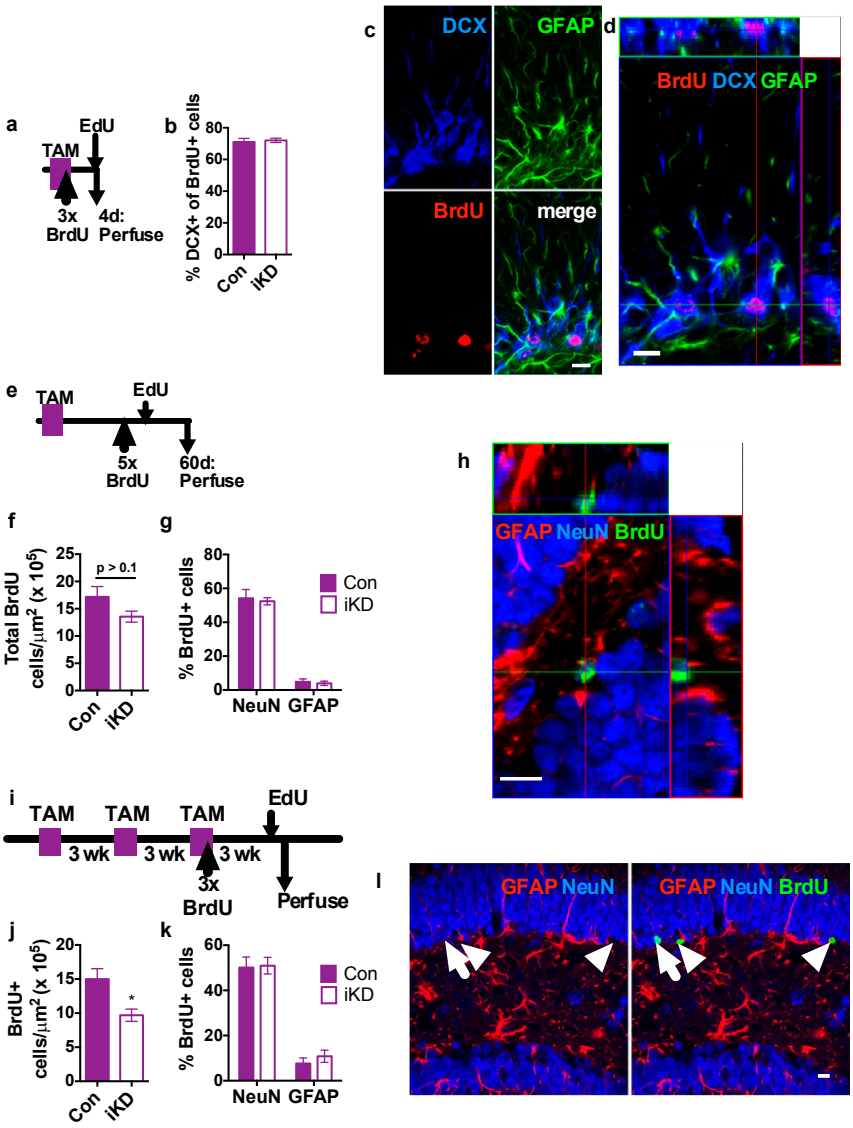


**Fig. S7.** NSPC-VEGF KD does not alter cell fate. (*A*) BrdU was injected one time per day for the last 3 d of TAM treatment. (*B*) Percentage of $BrdU^+$ cells expressing the early neuronal marker doublecortin (DCX) was not altered by VEGF-iKD. (*C*) Example merged z-stack of several $BrdU^+/DCX^+$ immature neurons. Very few $BrdU^+$ cells showed astrocytic $GFAP^+$ morphology at this time point. (Scale bar: 10 μm.) (*D*) Orthogonal image of a single 1-μm z-slice showing a $BrdU^+/DCX^+$ immature neuron. (Scale bar: 10 μm.) (*E*) BrdU was injected one time per day for 5 d 17–21 d after TAM. (*F*) Number of $BrdU^+$ cells surviving at 60 d was not different between groups. (*G*) Quantification of the percentage of $BrdU^+$ cells that coexpressed the mature neuronal marker NeuN or the astrocytic marker GFAP (and showed astrocytic morphology) revealed no difference in cell fate choice in con vs. VEGF-iKD mice. (*H*) Example orthogonal image of a $BrdU^+/NeuN^+$ new neuron from a mouse perfused 60 d after TAM. (Scale bar: 10 μm.) (*I*) BrdU was injected one time per day for 3d during the last TAM treatment. (*J*) VEGF-iKD reduced the total number of $BrdU^+$ cells labeled 3 wk before perfusion in the DG compared with control mice. $*P = 0.013$, *t* test. (*K*) Quantification of the percentage of those $BrdU^+$ cells that coexpressed the mature neuronal marker NeuN or the astrocytic marker GFAP (and showed astrocytic morphology) revealed no difference in cell fate choice in control vs. VEGF-iKD mice. (*L*) Example image of $BrdU^+/NeuN^+$ cell (arrow) or $BrdU^+$ cells with no other coexpressed marker (arrowheads). (Scale bar: 10 μm.) Data represent mean ± SEM.

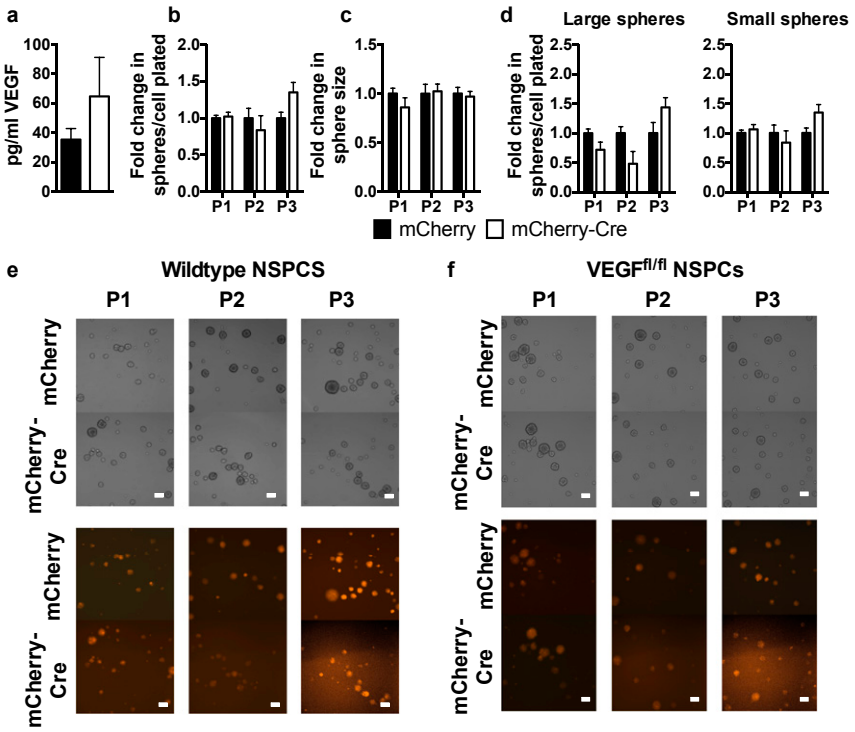


**Fig. S8.** WT NSPCs are not affected by mCherry-Cre expression. (*A*) Secretion of VEGF from WT NSPCs was not different between mCherry- and mCherry-Cre–expressing cells ($n = 3$ wells per group; one experiment). (*B*) WT NSPC total sphere number was not altered by mCherry-Cre expression (two-way ANOVA: interaction, $P = 0.11$; passage, $P = 0.11$; Cre, $P = 0.48$; $n = 3$ wells per group per experiment; two experiments). (*C*) WT NSPC sphere size was not altered by mCherry-Cre expression (two-way ANOVA: interaction, $P = 0.54$; passage, $P = 0.54$; Cre, $P = 0.43$). (*D*) mCherry-Cre expression did not change the number of large or small spheres in WT NSPCs (large, two-way ANOVA: interaction, $P = 0.0092$; passage, $P = 0.0092$; Cre, $P = 0.33$; small, two-way ANOVA: interaction, $P = 0.13$; passage, $P = 0.13$; Cre, $P = 0.41$; post hoc Holm–Sidak's multiple comparison tests within passage, all not significant). (*E*) Example bright-field (*Top*) and mCherry (*Bottom*) images of WT NSPCs expressing mCherry or mCherry-Cre. (*F*) Example bright-field (*Top*) and mCherry (*Bottom*) images of $VEGF^{fl/fl}$ NSPC-derived spheres. (Scale bars: 100 μm.) P1, passage 1; P2, passage 2; P3, passage 3.

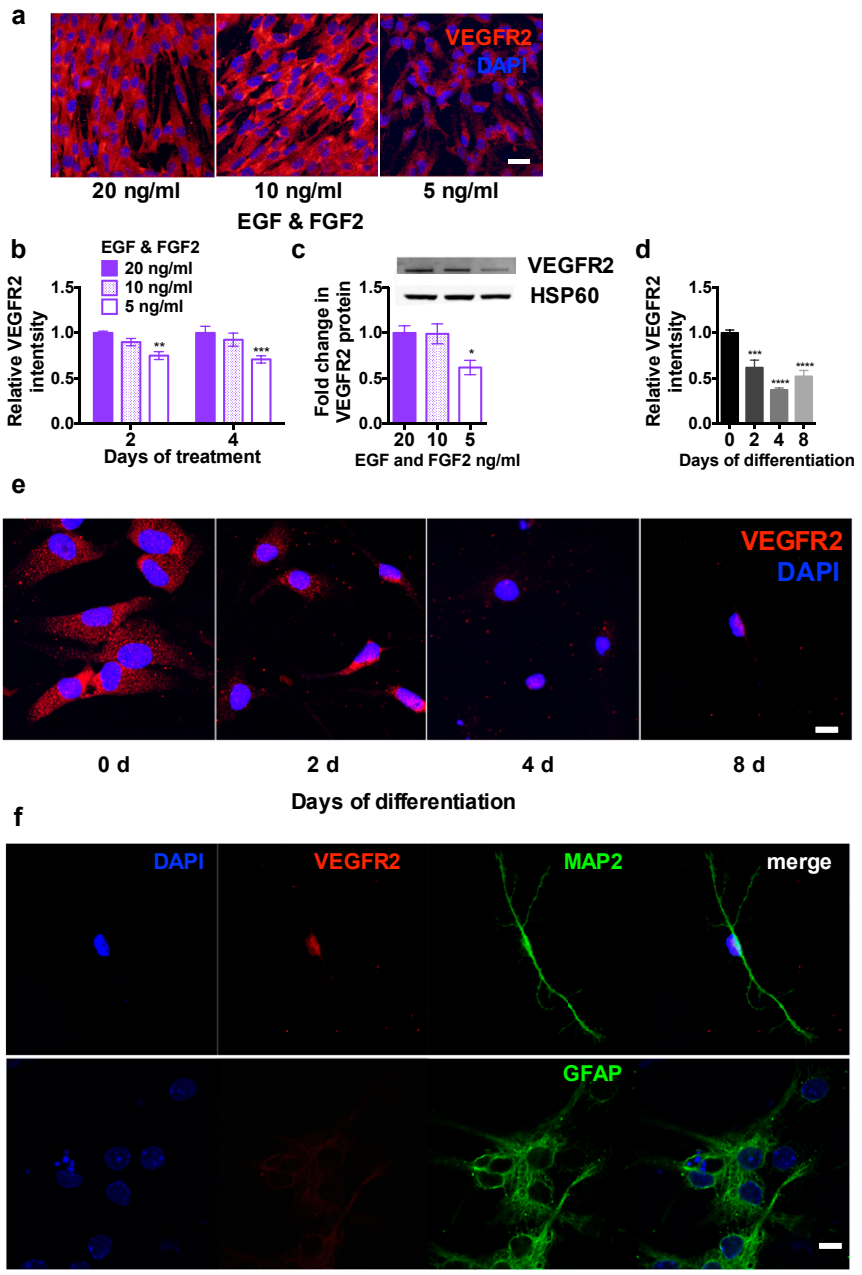


**Fig. S9.** Expression of VEGFR2 in NSPCs in vitro is environmentally regulated. (*A*) Example images of VEGFR2-ir in isolated NSPCs exposed to varying EGF and FGF2 concentrations for 4 d. (Scale bar: 10 μm.) (*B*) VEGFR2-ir decreased with decreasing EGF/FGF2 (two-way ANOVA: interaction, $P = 0.81$; day, $P = 0.91$; EGF/FGF2, $P < 0.0001$). $^{**}P < 0.01$; $^{***}P < 0.01$, post hoc Dunnett's comparisons to 20 ng/mL ($n$ = 2–3 wells per group per experiment, three experiments). (*C*) VEGFR2 protein (~150 kDa) measured by Western blot decreased with decreasing EGF/FGF2 treatment for 4 d (ANOVA, $P = 0.0117$; $n = 2$ wells per group per experiment; four experiments). $^{*}P < 0.05$, post hoc Dunnett's comparisons to 20 ng/mL. (*D*) VEGFR2-ir intensity decreased during differentiation (ANOVA, $P <$ 0.0001). $^{***}P < 0.001$; $^{****}P < 0.0001$, post hoc Dunnett's comparisons to 0 d ($n = 4$ wells per group per experiment; two experiments). (*E*) Example images of VEGFR2-ir during differentiation of NSPCs into neurons and astrocytes. (Scale bar: 10 μm.) (*F*) Example colabeling of NSPCs differentiated for 8 d into $MAP2^+$ neurons (*Top*) and $GFAP^+$ astrocytes (*Bottom*). The $MAP2^+$ neuron is the same cell shown in *E*, *Right*. (Scale bar: 10 μm.)

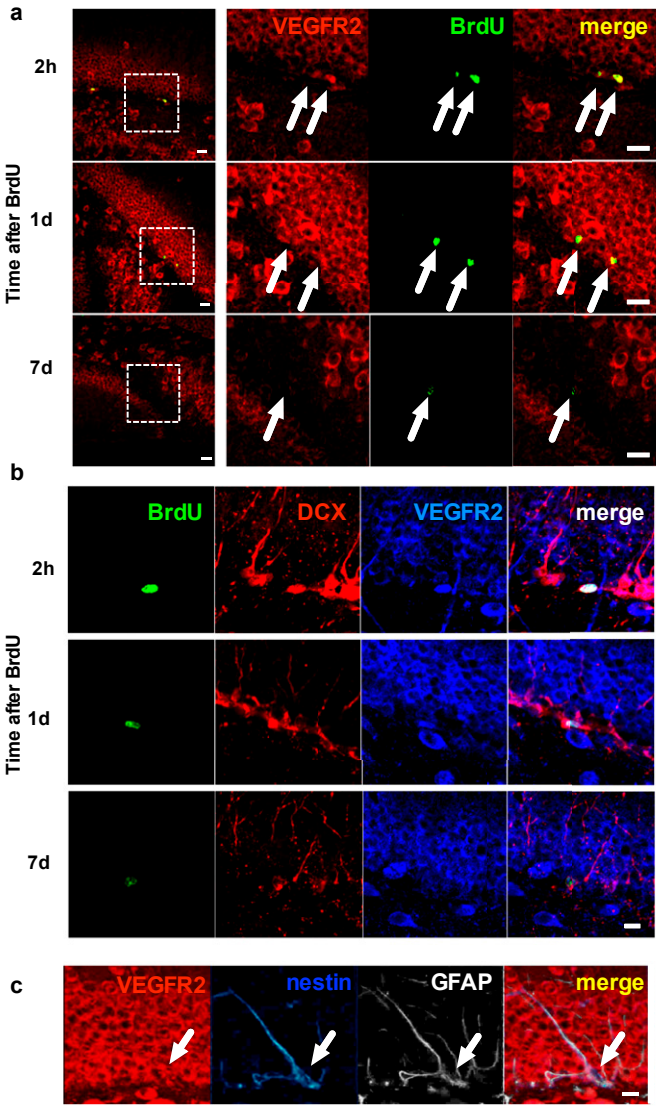


**Fig. S10.** NSPCs express VEGFR2 in vivo. (*A*) Example images of BrdU colocalization with VEGFR2 (white arrows) 2 h to 7 d after BrdU labeling. (*Right*) Dashed areas (*Left*) are shown. (*B*) Example images of BrdU colocalization with VEGFR2 and the immature neuron marker doublecortin 2 h to 7 d after BrdU labeling. Consistent with the nearly ubiquitous presence of VEGFR2-ir in the DG, $DCX^+$ new neurons showed VEGFR2-ir. (*C*) Example image of VEGFR2-ir in $nestin^+$/$GFAP^+$ RGL stem cell. (Scale bars: 10 μm.)

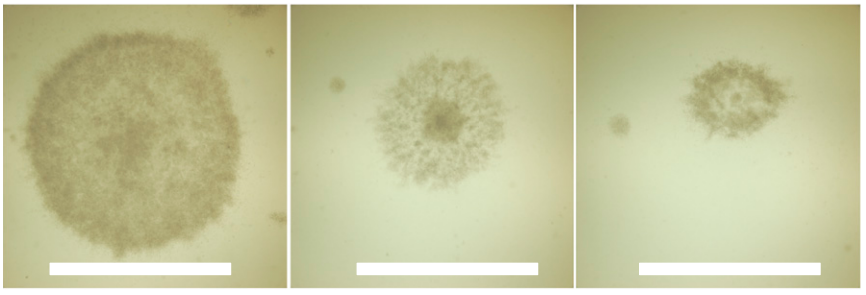

**Fig. S11.** Example colonies of different sizes in the NCFC assay. (Scale bars: 2 mm.)

**Table S1. Primer pairs used for qualitative and quantitative PCR and genotyping**

| Transcript | Primer 1 | Primer 2 | Use | Source |
|---|---|---|---|---|
| VEGF120 | 5′-agcacagcagatgtgaatgc | 5′-ttaatcggtctttccggtga | Qualitative PCR; 141-bp product | Designed by E.D.K. using Primer3 |
| VEGF164 | 5′-agcacagcagatgtgaatgc | 5′-ttaatcggtctttccggtga | Qualitative PCR; 272-bp product | Designed by E.D.K. using Primer3 |
| VEGF188 | 5′-agcacagcagatgtgaatgc | 5′-ttaatcggtctttccggtga | Qualitative PCR; 343-bp product | Designed by E.D.K. using Primer3 |
| VEGFR1 | 5′-tgaggagctttcaccgaact | 5′-tatcttcatggaggccttgg | Qualitative PCR | Designed by E.D.K. using Primer3 |
| VEGFR2 | 5′-gccacatggtctctctggtt | 5′-ggaatccataggcgagatca | Qualitative PCR | Designed by E.D.K. using Primer3 |
| Soluble Flt | 5′-aatggccaccactcaagatt | 5′-ttggagatccgagagaaaatg | Qualitative PCR | (1) |
| HSP60 | 5′-acctgtgacaacccctgaag | 5′-tgacacccttttcttccaacc | Real-time qPCR | Designed by E.D.K. using Primer3 |
| MAPK3 | 5′-tccgccatgagaatgttataggc | 5′-ggtggtgttgataagcagattgg | Real-time qPCR | Primer Bank: 21489933a1 |
| Actin | 5′-ggctgtattcccctccatcg | 5′-ccagttggtaacaatgccatgt | Real-time qPCR | Primer Bank: 6671509a1 |
| VEGF120 | 5′-agccagaaaaatgtgacaagc | 5′-tctttccggtgagaggtctg | Real-time qPCR | Designed by E.D.K. using Primer3 |
| VEGF164 | 5′-agccagaaaatcactgtgagc | 5′-gcgagtctgtgtttttgcag | Real-time qPCR | Designed by E.D.K. using Primer3 |
| VEGF188 | 5′-agcacagcagatgtgaatgc | 5′-tttcttgcgctttcgttttt | Real-time qPCR | Designed by E.D.K. using Primer3 |
| VEGFR2 | 5′-atctttggtggaagccacag | 5′-ccatgatggtgagttcatcg | Real-time qPCR | Designed by E.D.K. using Primer3 |
| Cre | 5′-gcggtctggcagtaaaaactatc | 5′-gtgaaacagcattgctgtcactt | Genotyping | The Jackson Laboratory |
| VEGF$^{fl}$ | 5′cctggccctcaagtacacctt | 5′-tccgtacgacgcatttctag | Genotyping | (2) |
| EYFP | 5′-aaagtcgctctgagttgttat | 5′-ggagcgggagaaatggatatg (WT)<br>5′-aagaccgcgaagagtttgtc (mutant) | Genotyping | The Jackson Laboratory |
| GFP (for VEGF-GFP) | 5′-tccttgaagaagatggtgcg | 5′-aagttcatctgcaccaccg | Genotyping | The Jackson Laboratory |

Qualitative PCR cycling protocol was 95 °C for 10 min, (95 °C for 20 s, 55 °C for 30 s, and 72 °C for 20 s) × 30, 72 °C for 7 min, and 4 °C hold. qPCR, quantitative PCR. Primer3 is available freely at biotools.umassmed.edu/bioapps/primer3_www.cgi.

1. Owen LA, et al. (2012) Morpholino-mediated increase in soluble Flt-1 expression results in decreased ocular and tumor neovascularization. *PLoS ONE* 7(3):e33576.
2. Gerber HP, et al. (1999) VEGF is required for growth and survival in neonatal mice. *Development* 126(6):1149–1159.

**Table S2. Antibodies used for immunohistochemistry, immunocytochemistry, and Western blots**

| Antibody | Vendor | Product no. | Use | Dilution | Pretreatment | Secondary/tertiary | Vendor, product no. |
|---|---|---|---|---|---|---|---|
| Rat anti-BrdU | Abcam | Ab6326 | IHC, ICC | 1:500 | DNA denaturation: 2N HCl, 30 min at 37 °C | Alexa Fluor 488 donkey anti-rat | Invitrogen, A21208 |
| Mouse anti–Flk-1 (A-3) (also known as VEGFR2) | Santa Cruz Biotechnology | Sc-6251 | IHC, ICC, Western blot | 1:100 (IHC), 1:200 (Western blot, ICC) | Antigen retrieval (IHC with BrdU only): 2N HCl, 30 min at 37 °C | Alexa Fluor 555 donkey anti-mouse (IHC); biotinylated donkey anti-mouse with streptavidin and Alexa Fluor 488, 555, or 647 (IHC); Alexa Fluor 488 donkey anti-mouse (ICC); Alexa Fluor 647 donkey anti-mouse (ICC) | Invitrogen, A-21432; Jackson Immuno-Research, 715-066-150 with Invitrogen S-32354, S-32355, S-21374; Invitrogen, A-21202, A-31571 |
| Rabbit anti-GFP | Invitrogen | A11122 | IHC | 1:1,000 | None | Biotinylated donkey anti-rabbit with streptavidin and Alexa Fluor 488 | Jackson Immuno-Research, 711-065-152; Invitrogen, S32354 |
| Goat anti-Sox2 | Santa Cruz Biotechnology | Sc-17320 | IHC | 1:1,000 | None | Alexa Fluor 647 donkey anti-goat | Invitrogen, A21447 |
| Goat anti-GFAP (C19) | Santa Cruz Biotechnology | Sc-6170 | IHC, ICC | 1:100 (IHC), 1:50 (ICC) | None | Alexa Fluor 647 donkey anti-goat (IHC); Alexa Fluor 555 donkey anti-goat (ICC) | Invitrogen, A-21447, A-21432 |
| Mouse anti-GFAP | Millipore | MAB360 | IHC | 1:500 | None | Alexa Fluor 555 donkey anti-mouse | Invitrogen, A-31570 |
| Rabbit anti-GFAP | DAKO | Z0334 | IHC | 1:2,000 | None | Alexa Fluor 555 donkey anti-rabbit; Alexa Fluor 488 anti-rabbit | Invitrogen, A-31573, A-21206 |
| Goat anti-doublecortin | Santa Cruz Biotechnology | Sc-8066 | IHC | 1:100 | None | Alexa Fluor 555 donkey anti-goat | Invitrogen, A-21432 |
| Rabbit anti-Ki67 | Abcam | Ab15580 | IHC | 1:100 | Antigen retrieval: 10 min, 10 mM NaCitrate + 0.5% Tween 20 in PBS at 95 °C | Alexa Fluor 555 donkey anti-rabbit | Invitrogen, A-31573 |
| Rabbit anti-Map2 | Abcam | Ab32454 | ICC | 1:1,000 | None | Alexa Fluor 488 anti-rabbit | Invitrogen, A-21206 |
| Chicken antinestin | Novus Biologics | NB100-1604 | IHC | 1:200 | Antigen retrieval: 10 min, 10 mM NaCitrate + 0.5% Tween 20 in PBS at 95 °C | Alexa Fluor 555 goat anti-chicken | Invitrogen, A-21437 |

**Table S2. Cont.**

| Antibody | Vendor | Product no. | Use | Dilution | Pretreatment | Secondary/tertiary | Vendor, product no. |
|---|---|---|---|---|---|---|---|
| Mouse anti-NeuN | Millipore | MAB377 | IHC | 1:500 | None | Alexa Fluor 555 donkey anti-mouse | Invitrogen, A-31570 |
| Rabbit anti-HSP60 | Abcam | Ab46798 | Western blot | 1:10,000 | None | IRDye 800CW goat anti-rabbit | Li-Cor, 926-32211 |
| Rat anti-CD31 | BD Biosciences | 550274 | IHC | 1:50 | Antigen retrieval: 30 min, trypsin ETDA at room temperature | Biotinylated donkey anti-rat with streptavidin and Alex Fluor 488 | Jackson Immuno-Research, 712-066-150; Invitrogen, S32354 |

ICC, immunocytochemistry; IHC, immunohistochemistry.